Journal of Peptide Science
J. Peptide Sci. **8**: 275–282 (2002)
Published online in Wiley InterScience (www.interscience.wiley.com). DOI: 10.1002/psc.388

A Comparison of Three- and Four-Helix Bundle TASP Molecules

ASHLEY S. CAUSTON and JOHN C. SHERMAN*

Department of Chemistry, 2036 Main Mall, Vancouver, B.C. Canada V6T 1Z1

Received 24 September 2001
Accepted 31 January 2002

Abstract: We have designed, synthesized and characterized three- and four-helix bundle template-assembled synthetic proteins (TASPs). The TASPs were synthesized using disulphide bonds between the peptides and either the cyclotribenzylene (CTB) template, or the cavitand (BOWL) template, to form the three- and four helix bundles, respectively. The TASPs were constructed using peptides that were linked via their *N*-termini (peptide CGGGEELLKKXEELLKKG, where X = L, I, Nle or V), or via their *C*-termini (peptide GEELLKKLEELLKKGGGC). Each TASP was assayed for its structure, stability, 'native-like' characteristics and whether it was a monomer in solution. All TASPs were found to be highly helical, and highly resistant to chemical denaturation using guanidine hydrochloride (GnHCl). Analysis of the GnHCl-induced unfolding curves of the different TASPs demonstrated stability differences based on the number of helices in the bundle, the end of the helix that was attached to the template, and the identity of the core amino acid. The TASPs all had molten-globule structure, which is (generally) consistent with a degenerate sequence in the core. The four-helix bundle TASPs appeared to be monomers in solution, whereas there is some evidence that the three-helix bundle TASPs are weakly self-associating.

Keywords: template assembled synthetic protein; TASP; three-helix bundle; four-helix bundle

INTRODUCTION

The three-dimensional structure of a protein is the result of a multitude of non-covalent interactions involving both the polypeptide backbone and its side chains [1]. A complete understanding of these forces would lead to the solution of the protein folding problem, i.e. prediction of a protein's structure from its amino acid sequence. Furthermore, *de novo* design of proteins with unique properties becomes possible with an understanding of the protein folding problem.

De novo proteins can be designed to simplify protein structure, and lead to a better understanding of the forces that are important to the higher levels of protein structure [2]. Three- and four-helix bundle proteins are common targets because of their relative simplicity. One major problem in the production of *de novo* proteins is that they have often resulted in molten-globule structures, which lack the conformational specificity (i.e. native-like structure) associated with natural proteins [3]. Increasing the diversity of the core amino acids in *de novo* designed proteins has led to folded structures that possess native-like structure [4].

The nature of the core amino acids has also been shown to be important to the quaternary structure

Abbreviations: BOWL, cavitand bowl; CD, circular dichroism spectroscopy (or spectrum); CTB, cyclotribenzylene; Da, daltons; DIPEA, N,N-diisopropylethylamine; DMA, dimethylactetamide; DMF, dimethylformanide; ESMS, electrospray mass spectrometry (or spectrum); GnHCl, guanidine hydrochloride; HPLC, high performance liquid chromatography; LSIMS, liquid secondary ionization mass spectrometry (or spectrum); TASP, template assembled synthetic protein; TFA, trifluoroacetic acid.

*Correspondence to: Dr John C. Sherman, Department of Chemistry, 2036 Main Mall, Vancouver, B.C. Canada V6T 1Z1.
Contract/grant sponsor: NSERC.

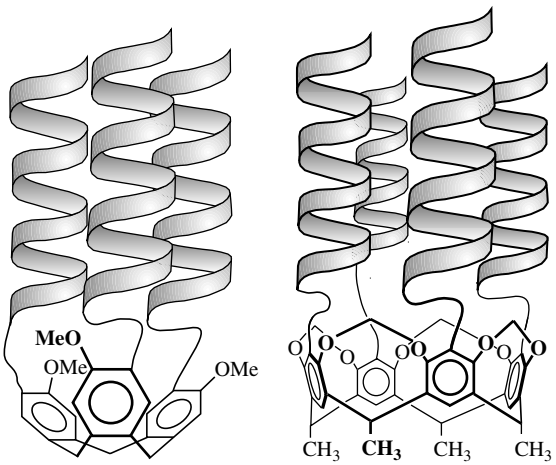

Figure 1 Schematic representation of three- and four-helix bundle TASPs.

of coiled-coil proteins. Subtle differences in the size, shape and position of amino acid side chains within the coiled-coil results in bundles that are either dimeric, trimeric, tetrameric, or exist as a multitude of oligomers [5].

The goals of this work are two-fold: First, to systematically investigate the features that are important to the production of native-like structure, and secondly, to investigate the features in an α-helix that would predispose it to be in a three- or a four-helix bundle structure. Thus, we studied three- and four-helix bundle structures using template assembled synthetic proteins (TASPs) [6] (Figure 1). Previously we reported the synthesis and characterization of four-helix bundles using a cavitand (BOWL) template [7], and three-helix bundles using a cyclotribenzylene (CTB) template [8]. From the work on the BOWL template in particular, we know the importance of the template-to-helix linker to the structure, conformational specificity, stability and association state of the TASP [7].

The peptides were designed to fold into amphiphilic α-helices; thus, bundling will occur between their hydrophobic faces in solution (see reference 8 for more details on the design of the TASPs). The BOWL and CTB templates (Figure 2) used for the present study contain benzylthiol moieties, which were the synthetic handles for the attachment of the peptide helices. Initially we used the peptide **N/L** (CGGGEELLKKXEELLKKG, X = L), where peptides were linked, via a disulphide bond, to either the CTB or BOWL template via a cysteine residue at its *N*-terminus (Figure 3), thus producing the three- and four-helix bundle TASPs **3N/L** and **4N/L**, respectively. The three-glycine 'spacer' between the template-bound cysteine residue and the 'helix' was found to be optimal for prevention of TASP self-association [9].

The helices in TASPs **3N/L** and **4N/L** were linked to the templates via their *N*-termini, and were compared with TASPs **3C/L** and **4C/L** (made with peptide **C/L**, GEELLKKLEELLKKGGGC), where the helices were linked via their *C*-termini. This would determine any end-capping effect of the CTB or BOWL template on (the stability of) the helical bundles.

The central amino acid in the core of the helix was then 'mutated' to assay its significance to the TASPs structure. Thus, the central Leu residue in peptide **N/L** (CGGGEELLKKXEELLKKG, X = L) was 'mutated' to isoleucine (peptide **N/I**, X = I), norleucine (peptide **N/Nle**, X = Nle) or valine (peptide **N/V**, X = V). These mutants were compared in terms of both stability and structural specificity (or 'native-like' structure).

MATERIALS AND METHODS

Synthesis

General. Chemicals (Aldrich or BDH) used for the synthesis were reagent grade except

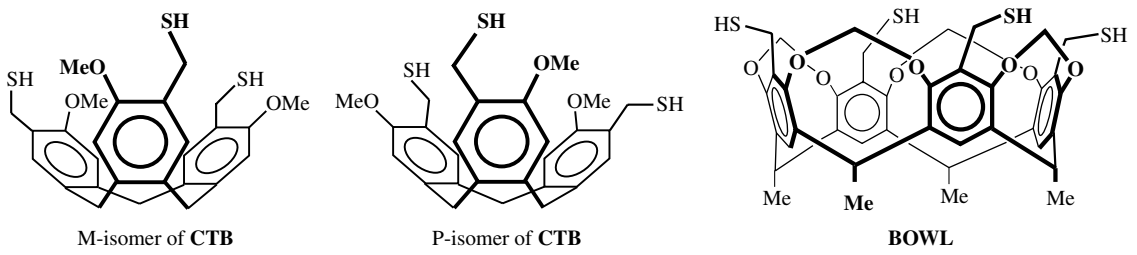

Figure 2 The CTB and BOWL templates used to make the three- and four-helix bundle TASPs. The CTB template exists as a pair of enantiomers.

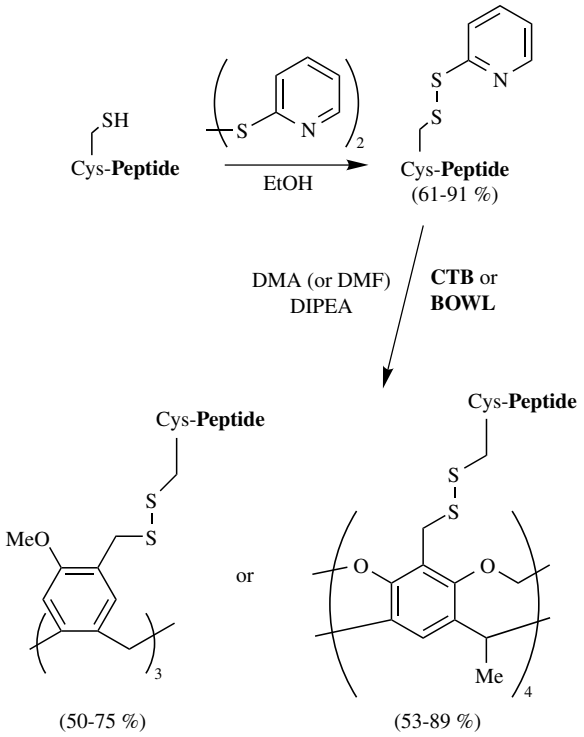

Figure 3 Synthesis of TASPs.

dimethylformamide (DMF) and dimethylacetamide (DMA) which were dried over 4 Å molecular sieves and degassed by bubbling dry N_2 through them for 5 min before use. CTB and BOWL were prepared as reported in the literature [10]. All peptides were prepared on a 0.25 mmol scale using an Applied Biosystems 431A peptide synthesizer using FastMoc™ chemistry with peptide synthesis grade (Advanced Chemtech, Aldrich or Richelieu Biotechnologies) reagents. The peptides and TASPs were purified using preparative scale C18 reverse phase HPLC (Perkin Elmer), using gradients of water (containing 0.1% TFA) and HPLC grade acetonitrile (containing 0.05% TFA); 229 nm was the wavelength monitored for product elution. Peptides were characterized by their correct mass using LSIMS performed on a Kratos Concept IIH32. TASPs were characterized using electrospray mass spectrometry (ESMS) run on a Perkin Elmer SCIEX API 300 LC/MS/MS system. All reported molecular weights were within ±2 Da of the calculated values.

Synthesis of activated peptides. The synthesis of **N(Spy)/L** represents a typical example of this reaction: Peptide **N/L** (20 mg, 11 µmol) in 3 ml of ethanol was added to a rapidly stirring solution of 2,2′-dipyridyl disulphide (12 mg, 55 µmol) in 2 ml of ethanol. The reaction was stirred at room temperature for 1 h. The ethanol was reduced to 1 ml volume *in vacuo* (such that the reaction mixture was still in solution), and the solution pipetted onto ice-cold diethyl ether. This formed a precipitate that was filtered and washed with diethyl ether. This solid was re-dissolved in water (1.5 ml) containing 0.1% TFA, filtered (0.45 µm nylon filter) and purified using preparative HPLC. Lyophilization (after removal of the acetonitrile *in vacuo*) resulted in 18 mg (75%) of **N(Spy)/L**. The yield of the activated peptides ranged from 61% to 91%, and the LSIMS gave masses consistent with calculated values.

Synthesis of disulphide linked TASPs. The synthesis of **4N/V** represents an example typical of this procedure: DIPEA (13 mg, 100 µmol) was added to a mixture of activated peptide **N(SPy)/V** (36 mg, 12 µmol) and BOWL (1.0 mg, 1.3 µmol) in DMA (5 ml) under a N_2 atmosphere. The reaction was stirred at room temperature for 1 h. The solvent was removed *in vacuo*, keeping the temperature of the water bath below 40 °C. The residue was re-dissolved in water (1.5 ml), filtered (0.45 µm nylon filter) and injected directly onto a preparative HPLC column. Lyophilization (after removal of the acetonitrile *in vacuo*) resulted in 9 mg (89%) of **4N/V**. The yield of the TASPs ranged from 50% to 89%, and the ESMS gave masses consistent with calculated values.

CD Spectroscopy

CD spectra were run on a Jasco J-710 spectropolarimeter using quartz cuvettes of 1 mm and 1 cm path length. The temperature was kept at 25 °C using a Haake FX 10 circulating bath. Samples were allowed 3 min to equilibrate to the desired temperature. Blanks were subtracted from the CD spectra, which were the average of three scans. Test samples for CD were prepared in duplicate or triplicate from stock solutions of known concentrations from amino acid analysis. The pH was measured using a Fisher Scientific Accumet® pH meter model 915. Guanidine hydrochloride denaturation experiments were performed by dilution of an 8.0 M solution of (10 mM, pH 7.0) GnHCl, using phosphate buffer (10 mM, pH 7.0). The exact concentration of the 8 M GnHCl stock solutions were determined by refractometry [11]. The disappearance of the CD signal at 222 nm was used to assess the degree of unfolding of the TASPs, the signal was 'normalized' to give values of 1.0 for a fully folded protein, and 0.0 for a fully unfolded protein.

Global Conformational Stability of ASPs: Calculated by Analysis of GnHCl-Induced Denaturation Curves

This method for analysis assumes that the TASP undergoes a fully reversible, cooperative, two-state unfolding process:

$$N \rightleftharpoons D$$

where N is the native state of the protein and D is the denatured state of the protein.

A non-linear least-squares method [12] was used for the analysis of the GnHCl-induced denaturation curves. This method estimates the pre- and post-transitional baselines, and assumes that the free energy of unfolding is a linear function of [GnHCl] according to the function:

$$\Delta G^{\circ}_{obs} = \Delta G^{\circ}H_2O - m[GnHCl]$$

where ΔG°_{obs} is the observed free energy of unfolding at a particular concentration of denaturant, $\Delta G^{\circ}H_2O$ is the free energy of unfolding in the absence of denaturant, m is change in ΔG°_{obs} with respect to [GnHCl] and [GnHCl] is the concentration of denaturant.

At a particular concentration of denaturant, ΔG°_{obs} can be calculated according to the following equation:

$$\Delta G^{\circ}_{obs} = -RT \ln K_{obs}$$

where R is the universal gas constant (1.987 cal K^{-1} mol^{-1}), T is the temperature (298 K for these unfolding experiments) and K_{obs} is an equilibrium constant for unfolding, calculated using:

$$K_{obs} = [D]/[N] = e^{-(\Delta G^{\circ}_{obs}/RT)} = e^{-((\Delta G^{\circ}H_2O - m[GnHCl])/RT)}$$
$$= f_D/f_N = (1 - f_N)/f_N$$

where f_D is the fraction of protein present in the unfolded state $= (1 - f_N)$ and f_N is the fraction of protein present in the folded state.

From the above equation we see that

$$(1 - f_N)/f_N = e^{-((\Delta G^{\circ}H_2O - m[GnHCl])/RT)}$$

and therefore that

$$f_N = e^{-((\Delta G^{\circ}H_2O - m[GnHCl])/RT)}/[1 + e^{-((\Delta G^{\circ}H_2O - m[GnHCl])/RT)}].$$

In order to account for pre- and post-transitional baselines, the data were fit to the following equation:

$$f_N = F_N(e^{-((\Delta G^{\circ}H_2O - m[GnHCl])/RT)}/ [1 + e^{-((\Delta G^{\circ}H_2O - m[GnHCl])/RT)}])(1 - a[GnHCl]) + F_U(1 - e^{-((\Delta G^{\circ}H_2O - m[GnHCl])/RT)}/ [1 + e^{-((\Delta G^{\circ}H_2O - m[GnHCl])/RT)}])$$

where F_N is the function of the folded state in the absence of GnHCl (nominally set to 0.9999), F_U is the function of the unfolded state (nominally set to 0.0001; in the cases where the TASP was not fully unfolded at 8 M GnHCl, the post-transitional baseline was estimated). a is a constant in the term accounting for the pre-transitional slope.

The values of $\Delta G^{\circ}H_2O$, m and a were determined by nonlinear least-squares analysis using KaleidaGraph 3.08 (Synergy Software). F_N and F_D were nominally set to values of 0.9999 and 0.0001, respectively (i.e. they were not determined by the least-squares analysis). All TASPs were treated as monomers when calculating their global stability. The presence of GnHCl, salt or methanol has been shown to disrupt (but not always overcome) the self-association of other members of our TASP family [7], therefore we made the assumption that they are monomers at the GnHCl concentration required for unfolding. However, any self-association of the TASPs around the unfolding transition point may introduce errors into these calculations.

NMR Spectroscopy

1D-^{1}H NMR spectra used to evaluate chemical shift dispersion were recorded at 500 MHz on a Brucker AMX500. Each sample (~0.3 mM) was dissolved in 45 mM phosphate buffer (90 : 10, H_2O : D_2O) at pH 7.0 and recorded at 25 °C. A relaxation delay of 1.0 s was used, during which time the water signal was saturated using a frequency-selective low-power decoupling pulse. The NMR spectra were processed using SwaN-MR 3.4.9 [13]. A convolution function was applied to remove the residual water signal.

Sedimentation Equilibrium Ultracentrifugation

Sedimentation equilibrium studies were performed by Dr Adam Mezo, in the laboratory of Professor Barbara Imperiali at the Massachusetts Institute of Technology. The data were collected on a temperature-controlled Beckman XL-A analytical

ultracentrifuge equipped with a photoelectric scanner, at the noted UV wavelength of 298 K, and a rotor speed of 33 000 rpm. Samples were allowed to equilibrate for 21–24 h (equilibrium was judged to have been reached when scans taken at 3 h intervals were duplicated). The data were analysed using MacNONLIN-PPC [14]. **4N/L** was found to exist as a monomer in buffer solution, whereas **3N/L** was found to exist in a monomer–dimer equilibrium with an association constant of 1500 ± 400 M^{-1}.

RESULTS AND DISCUSSION

Characterization of Structure

The ten TASPs presented here were all helical according to their CD spectra (Figure 4). The NMR spectrum of the monomeric peptide **N/L** was sharp (Figure 5), with concentration dependent chemical shift values for the N-H signals. This is consistent with rapid and reversible formation of helical bundles by peptide **N/L** [15]. The NMR spectra of all ten TASPs presented here were broad, especially in the N-H region (Figure 5 shows a typical NMR spectrum for a TASP); this is consistent with molten-globule structure. *De novo* designed proteins containing an all-leucine core often have been found to exhibit molten-globule structure [3]. However, other BOWL TASPs made in our group, which have different template-to-helix linkers than those presented here, appeared to manifest native-like structure when employing an all-leucine core [7]. It appears that the benzyl thiol linkage prevents native-like structure, while the aryl thiol linkage promotes it. Current efforts are underway to elucidate the source of these differences in conformational specificity.

Stability

When comparing helices that are linked via their *N*- versus *C*-termini, **4N/L** is more stable than **4C/L** by 3.4 kcal mol^{-1}, whereas **3N/L** is only marginally more stable than **3C/L** (Figure 6a and Table 1). This indicates that the BOWL template is a good *N*-cap for the helices, or that it destabilizes helices that are linked via their *C*-termini, or both. The CTB template does not display any significant end-capping effects. This observation in the differing end-capping abilities of the templates limits direct comparison between respective helical sequences in three- and four-helix bundle TASPs.

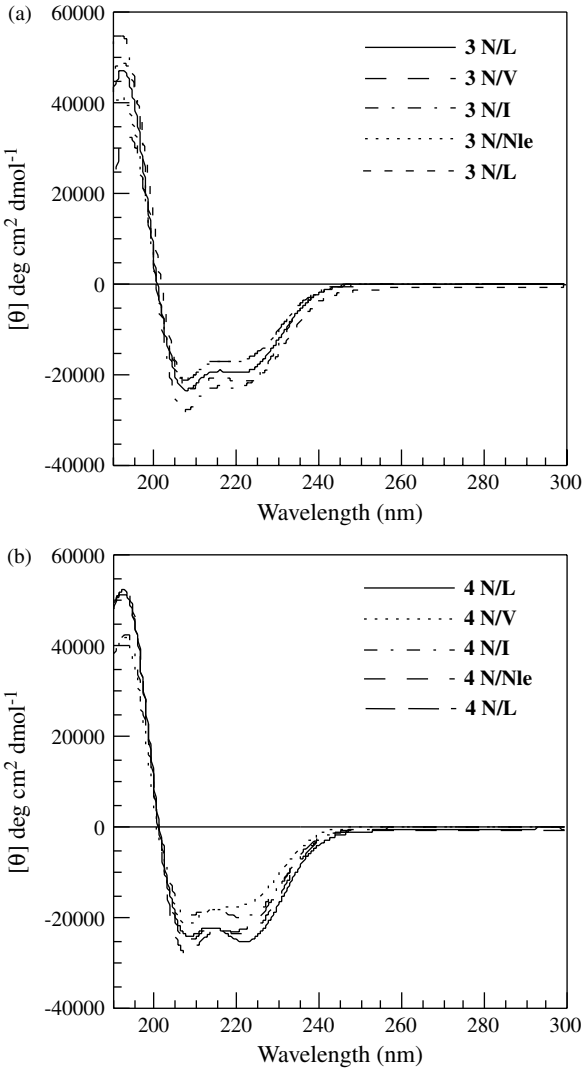

Figure 4 CD spectra of TASPs. Recorded in pH 7.0 phosphate buffer (10 mM) at 25 °C.

The superior *N*-capping ability of the BOWL is probably due to the presence of eight acetal oxygen atoms on the rim of the template (see Figure 2). The lone pair of electrons present in an oxygen atom may result in hydrogen bonding with an 'unsatisfied' backbone N-H at the *N*-terminus of the helix, thus stabilizing the overall structure.

Allowing for the difference in capping abilities, it still appears that the four-helix bundle TASPs are more stable than the three-helix bundle TASPs. This may be due to the increased burial of hydrophobic surface in the four-helix bundle; a feature that is known to increase the stability of proteins [1]. Also, the three-helix bundle TASPs contain helices that were designed to form four-helix bundles: Therefore

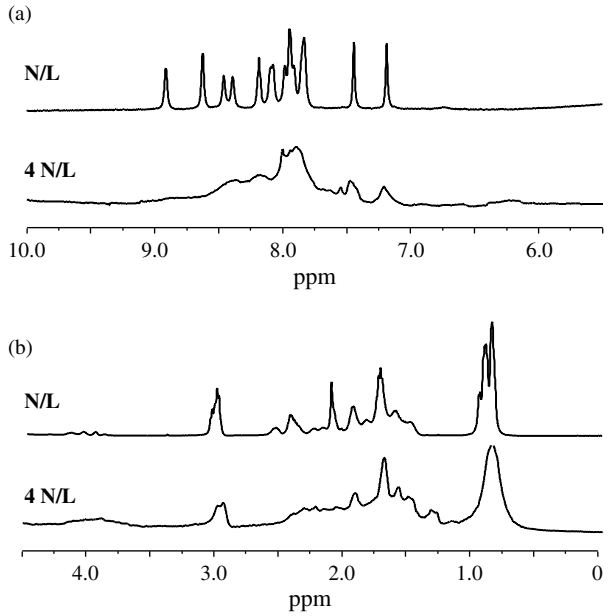

Figure 5 NMR spectra of peptide **N/L**, and TASP **4N/L** showing: (a) Downfield (N-H) region, 10.0–5.5 ppm (magnified); and (b) upfield (aliphatic) region, 4.5–0.0 ppm. Peptide (2.0 mM concentration) and TASP (~0.3 mM concentration) spectra were recorded at 298 K in 45 mM phosphate buffer (pH 7.0).

some of the hydrophobic 'core' may be exposed to the surface, decreasing the bundles' resistance to denaturation.

The three-helix bundle 'mutant' (Figure 6b and Table 1) with the greatest resistance to denaturation was the isoleucine analogue (order of stability is **3N/I**≈**3N/L**>**3N/Nle**>>**3N/V**). For the 'mutated' four helix-bundle TASPs (Figure 6c and Table 1), it appears that the leucine analogue has the greatest resistance to unfolding (order of stability is **4N/L**>**4N/I**≈**4N/Nle**>>**4N/V**). These observations are all within the context of a 'leucine-lined' hydrophobic core.

The TASPs containing the analogues of leucine (with four carbon atoms in the side chain) were more stable than those containing valine (which has three carbon atoms in its side chain). This observation is most likely due to the less buried hydrophobic surface in the valine-containing TASPs. For both the three- and four-helix bundle TASPs this equates to 0.9 kcal mol^{-1} per methylene-unit removed from the core (when comparing the β-branched **4N/I** with **4N/V**, and **3N/I** with **3N/V**). This energy value per methylene-unit removed from the core is consistent with similar observations made in larger proteins [16].

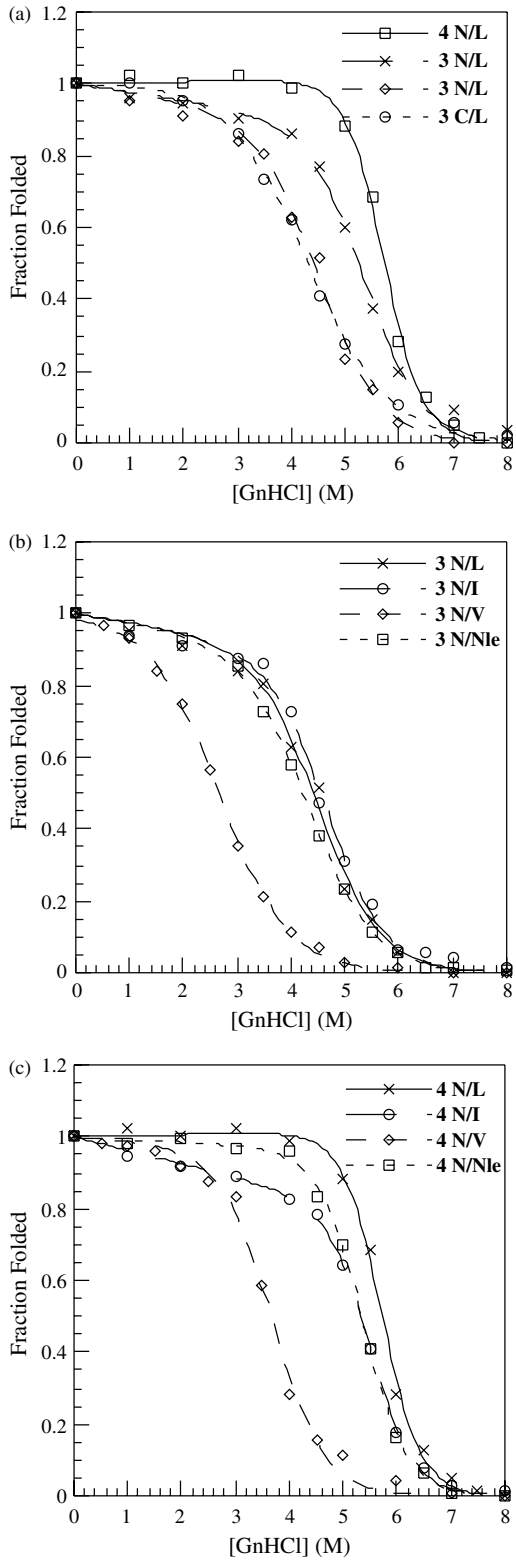

Figure 6 GnHCl-induced unfolding curves of TASPs. All spectra recorded in pH 7.0 phosphate buffer (10 mM) at 25 °C.

Table 1 Thermodynamic Evaluation of TASPs, Calculated from their GnHCl-induced Denaturation

TASP	Concentration (μM)	$[GnHCl]_{0.5}$ (M)	m (kcal mol^{-1} M^{-1})	$\Delta G°H_2O$ (kcal mol^{-1})	Per Helix $\Delta G°H_2O$ (kcal mol^{-1})
4N/L	3.0	5.7 ± 0.1	1.7 ± 0.1	9.4 ± 0.7	2.4
4N/I	2.8	5.3 ± 0.1	1.5 ± 0.2	8.2 ± 0.3	2.0
4N/V	3.2	3.6 ± 0.1	1.2 ± 0.1	4.6 ± 0.4	1.2
4N/Nle	2.7	5.4 ± 0.1	1.4 ± 0.2	7.8 ± 0.4	2.0
4C/L	2.5	5.2 ± 0.1	1.1 ± 0.1	6.0 ± 0.6	1.5
3N/L	4.0	4.4 ± 0.1	1.0 ± 0.1	4.7 ± 0.5	1.6
3N/I	3.2	4.8 ± 0.1	1.1 ± 0.1	5.0 ± 0.6	1.7
3N/V	3.1	2.6 ± 0.1	0.9 ± 0.1	2.4 ± 0.1	0.8
3N/Nle	3.9	4.2 ± 0.1	1.0 ± 0.1	4.1 ± 0.1	1.3
3C/L	3.6	4.3 ± 0.1	0.8 ± 0.1	3.7 ± 0.3	1.2

When comparing the stabilities of TASPs containing the leucine analogues (i.e. those made with peptides **N/L**, **N/I** and **N/Nle**), the helix secondary structure in all these bundles is affected by the same factors: Namely, the propensity of the amino acid to partake in an α-helix, and also the nature of the interactions between the residues at positions $i, i+4$ (which occupy the same side of the individual helices, the 'mutated' position in the core has two leucine residues that are four residues away in the sequence). Any other effects on the stability of the bundle result from tertiary interactions within the bundle. The TASPs were all molten-globules, but the size and shape of the core residues contributes to the global stability (tertiary structure) of the bundle.

Association State

All ten TASPs presented here demonstrated concentration independent GnHCl unfolding curves (data not shown), whereas the peptide alone demonstrated a concentration dependent GnHCl unfolding curve. This is consistent with all the TASPs existing as monomers in solution, and the peptide undergoing (concentration dependent) self-association. However, sedimentation equilibrium ultracentrifugation studies indicate that **4N/L** is a monomer in solution, whereas **3N/L** is in a monomer–dimer equilibrium. Low concentrations of GnHCl denaturant may overcome any inter-TASP self-association without detectable change in the secondary structure (unfolding in GnHCl is monitored by observation of the CD signal at 222 nm).

Self-association of **3N/L** may result from a helix sequence that is designed to form a four-, rather than a three-helix bundle. When 'forced' into a three-helix bundle, this sequence resulted in a TASP that underwent self-association; the helices in a three-helix bundle are always looking for that fourth helix to form the most favourable structure. The aggregation of 3N/L highlights the importance of design precision to higher levels of protein structure.

CONCLUSION

To overcome the association of the three-helix bundle TASPs we plan to design TASPs with a helix that favours the formation of a three-helix bundle. Furthermore, it may be interesting to look at this same sequence when it is 'forced' into a four-helix bundle. This work may allow us to discern some of the important design features when a helix is required to take part in a three- versus a four-helix bundle. Such design features that have not been investigated because there are few systems that can be used to embark on such a study.

Although all the TASPs studied had molten-globule structure, there were noticeable differences in the stabilities of both three- and four-helix bundles containing the 'mutated' central residue, which were attributed to the size and shape of the different side chains. These energy differences in a dynamic bundle structure may have significance as early folding intermediates. Current efforts are underway to change all the amino acids in the core of the TASPs, hopefully leading to a TASP with native-like structure.

It appears that the disulphide linker between a benzylthiol on the template and the side chain of a cysteine residue in the peptide is inferior to TASPs linked via the peptide backbone to an arylthiol template. TASPs containing a benzylthiol template linked to the peptide backbone also gave molten-globule structure [7]. We are currently investigating the benzyl versus disulphide components, and whether the sharper NMR spectra with the arylthiol-peptide backbone linker is due to native-like structure of fast-exchange of a molten-globule structure.

Acknowledgements

We thank NSERC for financial support. S. He for running the ESMS, A. Mezo for performing the sedimentation equilibrium experiments, C. Naumann for assistance with the NMR experiments and M. Fryzuk for the use of his HPLC.

REFERENCES

1. Creighton TE. *Proteins: Structures and Molecular Properties*, 2nd edn. W.H. Freeman & Co.: New York, 1992.
2. For a recent review on *de novo* designed proteins see: DeGrado WF, Summa C, Pavone V, Flavia N, Lombardi A. *De novo* design and structural characterization of proteins and metalloproteins. *Annu. Rev. Biochem.* 1999; **68**: 779–819.
3. Betz SF, Raleigh DP, DeGrado WF. *De novo* protein design: from molten globules to native-like states. *Curr. Opin. Struct. Biol.* 1993; **3**: 601–610.
4. Gibney BR, Rabanal F, Skalicky JJ, Wand AJ, Dutton PL. Iterative protein redesign. *J. Am. Chem. Soc.* 1999; **121**: 4952–4960.
5. Harbury PB, Zhang T, Kim PS, Alber T. A switch between two-, three-, and four-stranded coiled coils in GCN4 leucine zipper mutants. *Science* 1993; **262**: 1401–1407.
6. The TASP idea was pioneered by Mutter. Current efforts in this area are to create stable monomeric proteins with well-defined conformational specificity, and to incorporate functional groups to create functional proteins and enzymes. See: (a) Mutter M, Dumy P, Garrouste P, Lehmann C, Mathieu M, Peggion C, Peluso S, Razaname A, Tuchscherer G. Template assembled synthetic proteins (TASP) as functional mimetics of proteins. *Angew. Chem. Int. Ed. Engl.* 1996; **35**: 1481–1486. (b) Suich DJ, Mousa SA, Singh G, Liapakis G, Reisine T, DeGrado WF. *Bioorg. Med. Chem.* 2000; **8**: 2229–2241. (c) Rau HK, Haehnel W. *J. Am. Chem. Soc.* 1998; **120**: 468–476. (d) Futaki S. *Biopolymers* 1998; **47**: 75–81. (e) Wong AK, Jacobsen S, Winzor DJ, Fairlie DP. *J. Am. Chem. Soc.* 1998; **120**: 3836–3841. (f) Tahmassebi DC, Sasaki T. *J. Org. Chem.* 1998; **63**: 728–731.
7. Mezo AR, Sherman JC. Cavitands are effective templates for inducing stability and native-like structure in *de novo* four-helix bundles. *J. Am. Chem. Soc.* 1999; **121**: 8983–8994.
8. Causton AS, Sherman JC. Design of proteins using rigid organic macrocycles as scaffolds. *Bioorg. Med. Chem.* 1999; **7**: 23–27.
9. Causton AS. *Synthesis and Characterization of Template-Assembled Three- and Four-Helix Bundle Proteins*. PhD Thesis, University of British Columbia, Vancouver, Canada, 2001.
10. Keipert SJ. *Cavitands and 1,10-Phenanthroline-Containing Hosts for Alkali Cation Complexation*. PhD Thesis, University of California, Los Angeles, USA, 1985.
11. Pace CN. Determination and analysis of urea and guanidine hydrochloride denaturation curves. *Methods. Enzymol.* 1986; **131**: 266–280.
12. Santoro MM, Bolen DW. Unfolding free energy changes determined by the linear extrapolation method. 1. Unfolding of phenylmethanesulfonyl α-chymotrypsin using different denaturants. *Biochemistry* 1988; **27**: 8063–8068.
13. URL: http://www.qobrue.usc.es/jsgroup/swan/index.html
14. URL: http://www.beckman.com/Beckman/biosrch/BioLit/BioLitList.asp
15. Ciesla DJ, Gilbert DE, Feigon J. Secondary structure of the designed peptide alpha-1 determined by NMR spectroscopy. *J. Am. Chem. Soc.* 1991; **113**: 3957–3961.
16. Vlassi M, Cesarini G, Kokkinidis M. A correlation between the loss of hydrophobic core packing interactions and protein stability. *J. Mol. Biol.* 1999; **285**: 817–827.

